Journal of Engineering and Applied Sciences 13 (Special Issue 14): 11075-11080, 2018
ISSN: 1816-949X

Optoelectronic Characteristics of MnS/Si Photodiodes Prepared by Thermal Evaporation Technique

[1]Mazin H. Hasan, [2]Fuad T. Ibrahim and [3]Huda N. Abed
[1]Department of Physics, College of Science, University of Anbar, Baghdad, Iraq
[2]Department of Physics, College of Science, University of Baghdad, Baghdad, Iraq
[3]Al-Forat Vocational Preparatory School, Baghdad, Iraq

Abstract: In this research, Manganese Sulfide (MnS) thin films were deposited by thermal evaporation technique on glass or silicon substrates. The structural and morphological characteristics of these films were introduced. They also showed good transparency in the spectral range 300-900 nm. The MnS/Si heterojunctions were successfully fabricated at different temperatures and their electrical characteristics were determined and found to be very dependent on the structure of MnS films. The optoelectronic characteristics of these heterojunction photodiodes were also determined. Maximum spectral responsivity of 0.165 A/W was measured at 450 nm while maximum detectivity was about 2.359×10^{12} cm $Hz^{-1/2}W^{-1}$ at 450 nm. This research is good attempt to fabricate MnS/Si heterojunction detectors with relatively good characteristics and low production cost.

Key words: Photodiodes, thermal evaporation, MnS, optoelectronics, transparency, evaporation

INTRODUCTION

Manganese sulfide is a broad energy gap (3.1 eV) dilute magnetic semiconducting material that is of potential regard in short wavelength optoelectronic applications such as photodetectors, selective coatings, solar cells, sensors, optical mass memories (Eckertova, 1977; Sadoon and Sharma, 2017). Therefore, the optical properties of MnS thin films are significant for many applications. Manganese Sulfide (MnS) thin films or powders can be found in several polymorphic forms: the rock-salt type structure (α-MnS) which is the most common form. By low temperature growing techniques, it crystallizes into the zinc-blende (β-MnS) or wurtzite (λ-MnS) structure (O'Brien *et al*., 2000; Fan *et al*., 2003; Piriou *et al*., 1994; Tappero *et al*., 1997). Manganese and its compounds have interesting electronic and semiconductor properties that attract major attentions in technological applications. Recently, metal chalcogenide thin film materials have opened a new area in the field of electronic applications. Their structural, electrical and optical properties can be controlled by changing the crystallite size and/or film thickness depending upon the deposition conditions (Lokhande *et al*., 1998; Kobayashi *et al*., 1995). MnS thin films has been prepared and grown by different methods such as radiofrequency sputtering (An *et al*., 2003; Mayen-Hernandez *et al*., 2003), hydrothermal (David *et al*., 2002; Reddy *et al*., 2008), Molecular Beam Epitaxy (MBE) and Chemical Bath Deposition (CBD). In general, the properties of thin films are critically dependent on preparation method or technique.

In this study, MnS thin films are prepared by high-vacuum thermal evaporation technique. The structural, morphology and optical properties of these films are introduced. As well, the optoelectronic characteristics such as current-voltage characteristics in both dark and light, spectral responsivity, specific detectivity and minority carrier lifetime of MnS/Si heterojunction were determined to assess this heterojunction as photodiode.

MATERIALS AND METHODS

Experimental work: The glass slide and silicon wafer were used as substrates on which thin MnS films were deposited. The glass slide was cut into 1.5×1.5 cm substrates. Prior to deposition process, they were thoroughly cleaned using a diluted solution of chemical detergents to remove impurities and residuals on their surfaces. Similarly, silicon wafer was cleaned with alcohol in ultrasonic bath to remove impurities and residuals from its surface. Then, it was rinsed in HF (10%) for 5 min to remove the original oxides.

The bottom side of silicon wafer was coated with a 200 nm thick aluminum layer for electrical measurements. This layer was deposited by evaporation of high purity (99.99%) aluminum wire in vacuum starting at 10^{-5} Torr.

Corresponding Author: Fuad T. Ibrahim, Department of Physics, College of Science, University of Baghdad, Baghdad, Iraq

The Manganese Sulfide (MnS) films were deposited by the same thermal evaporation system in vacuum starting at 2×10^{-5} Torr using a molybdenum boat. The evaporation rate was 23.5 nm/min and the film thickness was measured by the interference method.

The glass substrate was placed directly above the MnS source at a distance of about 18 cm. The structures of prepared samples were determined by Shimadzu XRD-6000 X-ray diffractometer (CuKα), the Fourier-Transformation Infrared (FTIR) spectroscopy was carried out by Shimadzu 8400S instrument, scanning electron microscopy was carried out by JEOL JSM-5600 SEM instrument, Transmission Electron Microscopy (TEM) was carried out by Philips CM10 PW6020, Atomic Force Microscopy (AFM) was carried out by Angstrom AA3000 instrument and the UV-Visible spectroscopy was carried out by Cary 100 Conc plus UV-Vis spectrophotometer.

RESULTS AND DISCUSSION

Figure 1 shows the XRD patterns of as prepared MnS thin films and thermally annealed films (at 150°C) deposited on glass substrates. It revels a strong peak of MnS in both as-prepared and annealed samples at 2θ of 29.66 and 29.692°, respectively. These values are corresponding to the (111) orientation (Trivedi *et al*., 2015). All diffraction peaks in Fig. 1 indicate the cubic structure of the prepared samples with no trail of hexagonal or other faces. The crystallite size (D) is given by Eq. 1:

$$D = \frac{k\lambda}{\beta\cos(\theta)} \quad (1)$$

where, the λ is the wavelength of x-ray used for diffraction, β is the Full Width at Half Maximum (FWHM) of the characteristic spectrum in radians, k is the Scherrer's constant (1>k>0.89). The crystallite size was fund to be 10.3 nm which is in agreement with the grain size determined by AFM.

Figure 2 shows 3D AFM image and granularity accumulation distribution of MnS nanostructures in the thin film sample deposited on glass substrate. The substrate is well-covered with MnS nanostructures those distributed uniformly on the surface. It is obvious from this figure that the nanostructures have small ordered particles with semispherical shape. The average grain size was estimated with the aid of appropriate software to be 70.01 nm while the values of average ($R_{ave.}$) and root mean square (R_{rms}) roughness were 2.01 and 2.37 nm, respectively.

Figure 3 represents the FTIR spectrum of MnS thin film sample and shows several significant peaks of absorption. The broad absorption band in the region of 600-2100 cm^{-1} is assigned to Mn-S stretching mode. The spectra of the annealed samples showed absorption bands at 620, 892 and 1123 cm^{-1}, those are attributed to O-H stretching vibration.

Figure 4 shows the transmission spectrum as a function of wavelength for MnS thin films deposited on

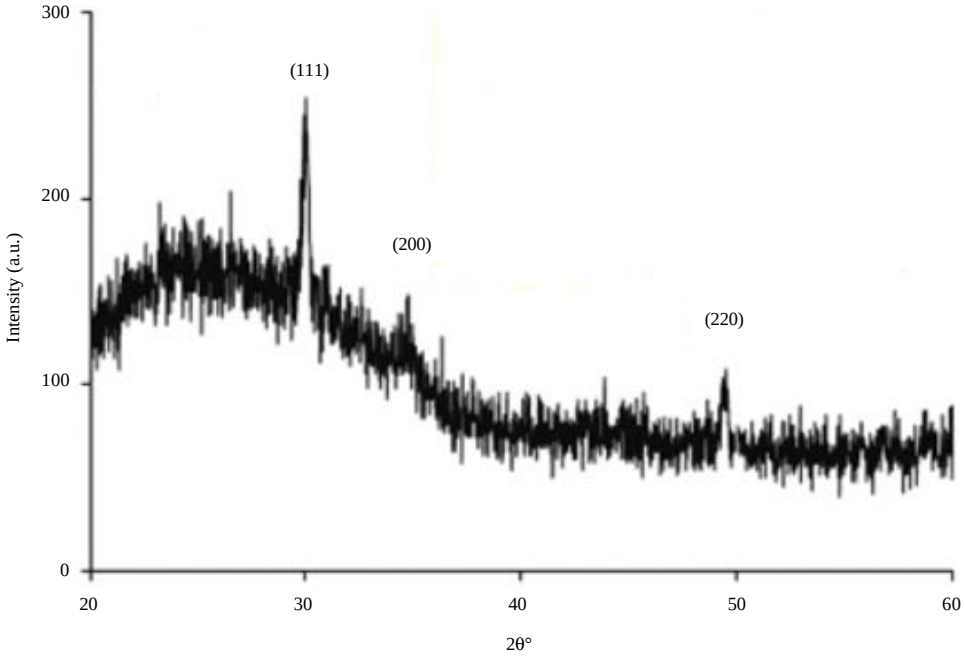

Fig. 1: The XRD pattern of the MnS films prepared in this research

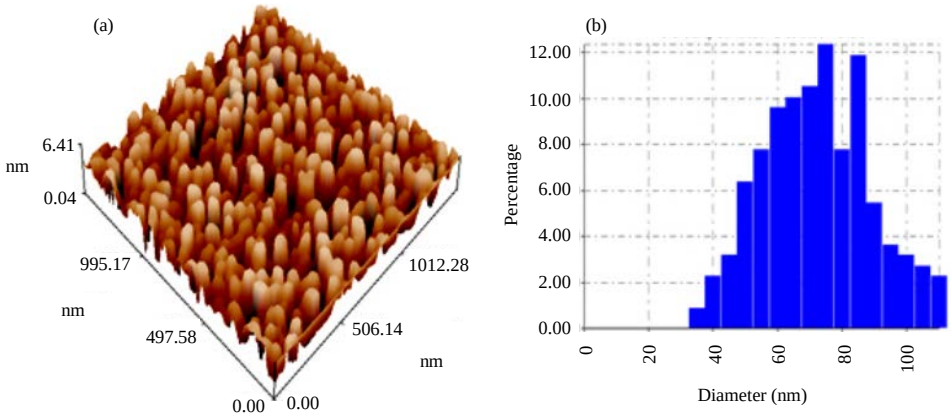

Fig. 2a, b): The 3D AFM image and granularity accumulation distribution of the MnS sample

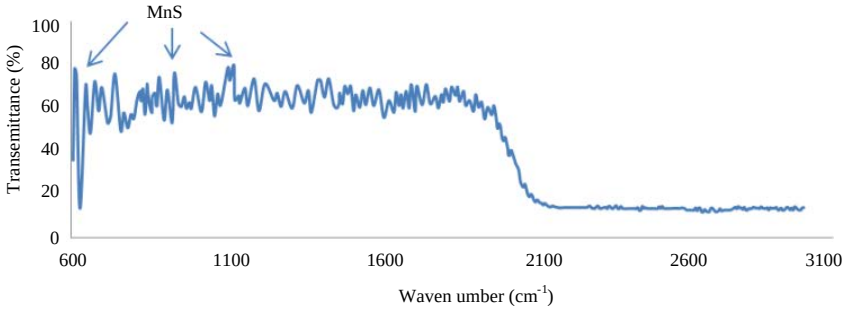

Fig. 3: The FTIR spectrum of MnS thin film prepared in this research

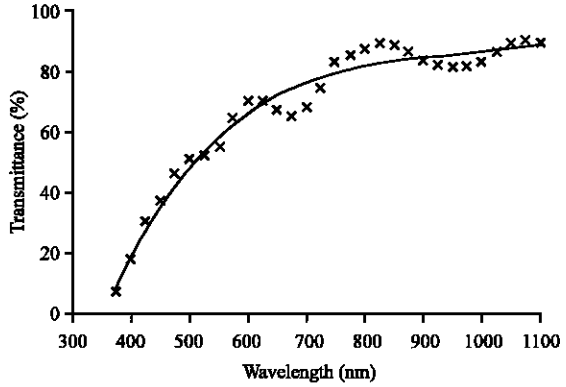

Fig. 4: Optical transmittance of MnS thin films

glass substrates. It is obvious that these films are good transparent in the spectral range 600-1000 nm. The transmission sharply increases in the UV region due to the absorption by nano-sized particles. The transmission was measured to be 80-90% in the spectral range 750-1100 nm which represents the Near-Infrared Region (NIR) while the maximum transmittance (90.1%) was recorded at 1075 nm. This makes these MnS films good candidate as window material for solar cells. The optical energy band gap of MnS was calculated by the relation (An *et al*., 2003):

$$\alpha h\nu = a\left(h\nu - E_g\right)^n \quad (2)$$

Where:

α = The absorption coefficient
A = A constant
ν = The transition frequency and the exponent
n = Characterizes the nature of band transition

where, n = 1/2 and 3/2 correspond to direct allowed and forbidden transitions, respectively and n = 2 and 3 correspond to indirect allowed and forbidden transitions, respectively. Figure 5 shows the relation between $(\alpha h\nu)^2$ and photon energy ($h\nu$) from which the energy band gap of MnS thin films determined by extrapolating the linear part of the curve toward the photon energy axis. The energy band gap was found to be about 2.85 eV.

Figure 6 shows the Photoluminescence (PL) emission spectrum of MnS thin film sample at room temperature with an excitation source of 400 nm. A single sharp broad emission peak is centered at 3000 nm.

Figure 7 shows the dark I-V characteristics of MnS/Si heterojunction in both forward and reverse bias conditions. The forward current of this heterojunction is very low at a bias voltage lower than 1.2 V.

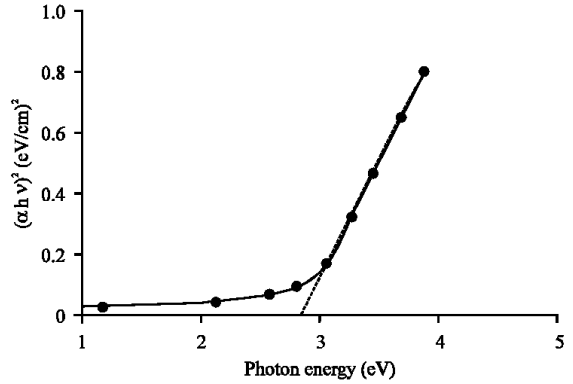

Fig. 5: Plot of $\alpha h\nu^2$ versus $h\nu$ of as-prepared MnS thin films

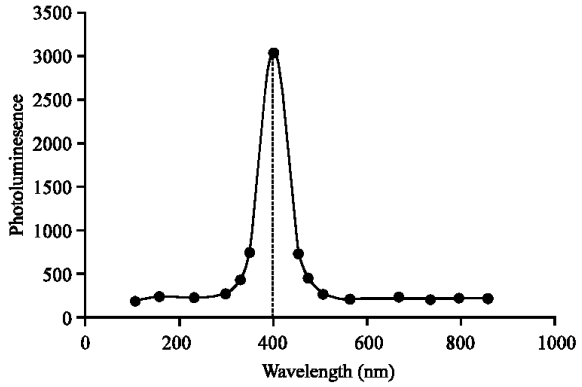

Fig. 6: The Photoluminescence (PL) spectrum of MnS sample

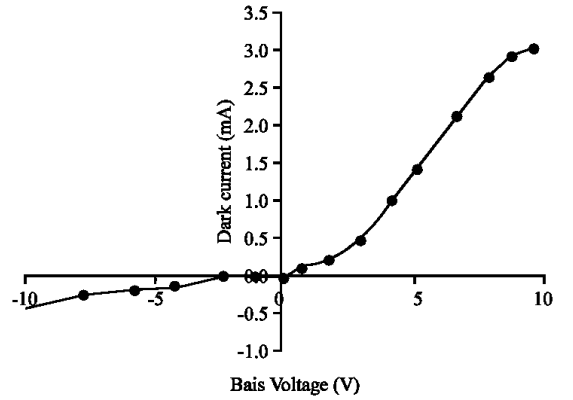

Fig. 7: The I-V characteristics of the MnS heterojunction under forward and reverse bias conditions

The current is known as the recirculation current at low voltages only. It is created when each excited electron forms the equivalence range of the conductive band. The second high voltage zone represents the area of propagation or bending which depends on serological

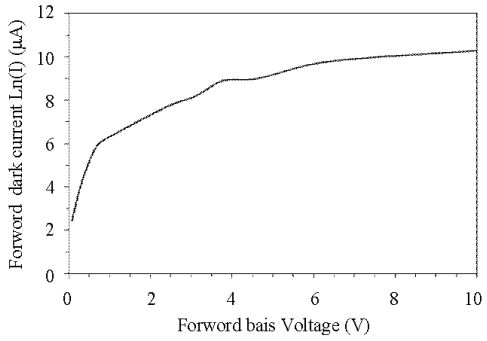

Fig. 8: Variation of forward dark current (lnI) with forward bias voltage of MnS heterojunction

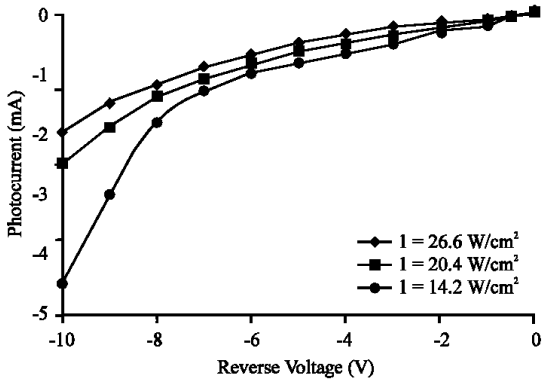

Fig. 9: The I-V characteristics under forward reverse bias for MnS heterojunction

resistance. In this region, the bias voltage can deliver electrons with enough energy to penetrate the barrier between the two sides of the junction.

Figure 8 shows the variation of ln(I) with bias voltage of MnS/Si heterojunction. The ideality factor of the heterojunction was estimated to be 4.8.

Figure 9 shows the variation of photocurrent with reverse bias voltage under different illumination intensities using tungsten lamp (14.2, 20.4 and 26.6 W/cm^2). It can be observed that the inverse current value in a standard voltage of hetero-diode meters under luminance is higher than that in the dark and can be seen from Fig. 9 that the current value in a certain voltage of the opposite connectors under the illumination is higher than in the darkness, generation of the current caused by the carrier due to electron-hole production due to light absorption. This behavior produces useful information about electron hole pairs which are effectively generated in the link by the photons that occur.

Figure 10 shows a linear relation between inverse of squared Capacitance ($1/C^2$) and the reverse bias voltage for MnS/Si heterojunction which indicates that it is an

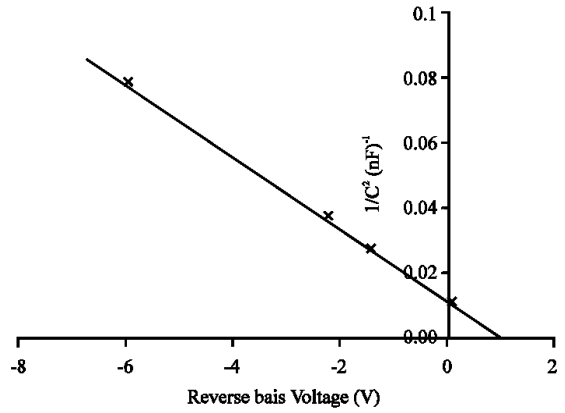

Fig. 10: Plot of $1/C^2$ versus reverse bias voltage of MnS photodieode

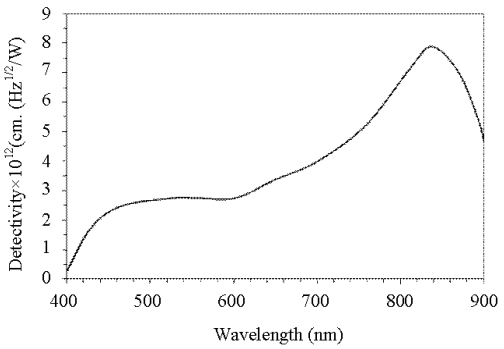

Fig. 11: The detectivity of the MnS photodiode as a function of wavelength

abrupt junction. The built-in potential (V_{bi}) was determined by extrapolating the line to intersect with the voltage axis and found to be 1.2 V.

Figure 11 shows the variation of specific Detectivity (D^*) with incident wavelength for the MnS/Si heterojunction. It consists of two reaction peaks, the first peak is at 450 nm due to the absorption margin of MnS nanoparticles while the second is located around 840 nm as a result of edge absorption of the silicon substrate. The maximum value of detectivity due to MnS was 2.359×10^{12} cm.Hz^{-1}.W^{-1} at 450 nm.

CONCLUSION

The MnS/Si heterojunction was successfully fabricated by using thermal evaporation technique. This heterojunction was thermally annealed at 150°C in order to enhance its electrical and optical properties. The I-V characteristics of this heterojunction are strongly dependent on the structure. Maximum spectral responsivity and specific detectivity of this heterojunction were determined to be 0.165 A/W and 2.359×10^{12} cm Hz^{-1}.W^{-1} at 450 nm, respectively. These results make the photodiode based on this heterojunction efficient for optoelectronic applications.

REFERENCES

An, C., K. Tang, X. Liu, F. Li and G. Zhou *et al*., 2003. Hydrothermal preparation of α-MnS nanorods from elements. J. Cryst. Growth, 252: 575-580.

David, L., C. Bradford, X. Tang, T.C.M. Graham and K.A. Prior *et al*., 2002. Growth of zinc blende MnS and MnS heterostructures by MBE using ZnS as a sulphur source. Proceedings of the International Conference on Molecular Bean Epitaxy, September 15-20, 2002, IEEE, San Francisco, California, USA., pp: 261-262.

Eckertova, L., 1977. Physics of Thin Films. Plenum Press, New York, USA., ISBN-13:978-1-4615-7591-7, Pages: 254.

Fan, D., X. Yang, H. Wang, Y. Zhang and H. Yan, 2003. Photoluminescence of MnS thin film prepared by chemical bath deposition. Phys. B. Condens. Matter, 337: 165-169.

Kobayashi, M., T. Nakai, S. Mochizuki and N. Takayama, 1995. Validity of the Sugano-Tanabe diagram for band states in MnO and MnS under high pressure. J. Phys. Chem. Solids, 56: 341-344.

Lokhande, C.D., A. Ennaoui, P.S. Patil, M. Giersig and M. Muller *et al*., 1998. Process and characterisation of chemical bath deposited manganese sulphide (MnS) thin films. Thin Solid Films, 330: 70-75.

Mayen-Hernandez, S.A., S. Jimenez-Sandoval, R. Castanedo-Perez, G. Torres-Delgado and B.S. Chao *et al*., 2003. Preparation and characterization of polycrystalline MnS thin films by the RF-sputtering technique above room temperature. J. Cryst. Growth, 256: 12-19.

O'Brien, P., D.J. Otway and D. Smyth-Boyle, 2000. The importance of ternary complexes in defining basic conditions for the deposition of ZnS by aqueous chemical bath deposition. Thin Solid Films, 361: 17-21.

Piriou, B., J. Dexpert-Ghys and S. Mochizuki, 1994. Time-resolved-photoluminescence spectra of MnO and MnS. J. Phys. Condens. Matter, 6: 7317-7327.

Reddy, D.S., K.N. Rao, K.R. Gunasekhar, N.K. Reddy and K.S. Kumar *et al*., 2008. Annealing effect on structural and electrical properties of thermally evaporated $Cd_{1-x}Mn_xS$ nanocrystalline films. Mater. Res. Bull., 43: 3245-3251.

Sadoon, A. and R. Sharma, 2017. Studies and characterization of nanostructured MnS thin film prepared by chemical bath deposition. Intl. J. Pure Appl. Phys., 13: 241-248.

Tappero, R., P. D'Arco and A. Lichanot, 1997. Electronic structure of α-MnS (alabandite): An AB initio study. Chem. Phys. Lett., 273: 83-90.

Trivedi, M.K., R.M. Tallapragada, A. Branton, D. Trivedi and G. Nayak *et al*., 2015. Characterization of atomic and physical properties of biofield energy treated manganese sulfide powder. Am. J. Phys. Appl., 3: 215-220.